

# A robust LMI-based pitch controller for large wind turbines

H.M. Hassan\*, A.L. ElShafei, W.A. Farag, M.S. Saad

Electrical Power and Machines Department, Faculty of Engineering, Cairo University, El-gamea Street, Giza 12613, Egypt

## ARTICLE INFO

### Article history:

Received 8 July 2011

Accepted 30 December 2011

Available online 31 January 2012

### Keywords:

Pitch control

LMI

$H_\infty$  problem

$H_2$  problem

Polytopic system

Pole clustering

## ABSTRACT

This paper utilizes the linear matrix inequalities' techniques (LMI) for designing a robust collective pitch controller (CPC) for large wind turbines. CPC operates during up rated wind speeds to regulate the generator speed in order to harvest the rated electrical power. The proposed design takes into account model uncertainties by designing a controller based on a polytopic model. The LMI-based approach allows additional constraints to be included in the design (e.g.  $H_\infty$  problem,  $H_2$  problem,  $H_\infty/H_2$  trade-off criteria, and pole clustering). These constraints are exploited to include requirements for perfect regulation, efficient disturbance rejection, and permissible actuator usage. The proposed controller is combined with individual pitch controller (IPC) that reduces the periodic blade's load by alleviating once per revolution (1P) frequency fatigue loads. FAST (Fatigue, Aero-dynamics, Structures, and Turbulence) software code developed at the US National Renewable Energy Laboratory (NREL) is used to verify the results.

© 2012 Elsevier Ltd. All rights reserved.

## 1. Introduction

The use of wind power is increasing rapidly. At the same time the need for better cost effectiveness of wind power plants has stimulated growth in wind turbines' size and power. In above-rated wind conditions, the goals for turbine operation change from control of generator torque for maximum power tracking to those of regulating power at rated levels with mitigating fatigue loading on the turbine structure. An ordinary PI pitch controller regulates the generator speed without taking into consideration the unstructured dynamics of the blades, the drivetrain nor the tower. The nonlinear variation of rotor torque with wind speed and the pitch angle are typically not considered in design. Further, the pitch actuator also has restricted limits on pitch angle and pitch rate [1]. Other challenging problems are the presence of nonlinearities in the system dynamics, and the continuous change of the operating points during operation. All previous reasons motivate the need for robust pitch controller that provides an accepted performance, and disturbance rejection at different operating points within the allowed actuator constrains. In this paper, a multi-objective collective pitch controller will be designed using LMI techniques for generator speed regulation.

Another objective is to reduce the structural mechanical loads by using IPC. This should be fulfilled within the permissible range and rate of the pitch angle of the actuator. The importance of load reduction becomes vital as turbines become larger and more

flexible. When the turbine blade sweeps, it experiences changes in wind speed due to wind shear, tower shadow, yaw misalignment and turbulence. These variations lead to (1P) large component in the blade loads, it's essential to design (IPC) to cancel this component [2].

Pitch controller is designed using  $H_\infty$  technique in [3,4]. In these papers, the controller main objective is to regulate the speed by improving disturbance rejection. The required control effort isn't considered in the design. In [5], it is proposed to design gain scheduled feedback/feed forward CPC for speed regulation combined with IPC for load reduction. Also in [6], optimal LQG feedback/feed forward CPC is proposed for speed regulation combined with IPC for load reduction. Combined CPC with IPC is proposed in [7] both as PI controllers. In [5–7], all the proposed controllers is based on a single linearized model, which only reflects one single operating point. A multi-objective ( $H_2/H_\infty$ ) pitch controller is proposed in [8], but it doesn't provide ( $H_2/H_\infty$ ) trade-off criteria. It also doesn't consider improving the transient response at different operating points. In our proposed work in this paper, an LMI-based CPC is considered. The controller design constraints include  $H_\infty$  problem for better speed regulation, and  $H_2$  problem for optimizing control action with performance. The design also addresses  $H_\infty/H_2$  trade-off criteria for the optimization of the two previous problems. Pole clustering for improving transient response is also considered. The controller is based on a polytopic model to overcome model uncertainty at different operating points. CPC is combined with IPC to mitigate mechanical fatigue loads.

\* Corresponding author. Tel.: +20 102241739.

E-mail address: [hussain\\_hassan@ieee.org](mailto:hussain_hassan@ieee.org) (H.M. Hassan).

**Table 1**  
Wind turbine specifications.

Hub height	90 m
Rotor diameter	126 m
Cut in, rated, cut out wind speed	3 m/s, 11.4 m/s, 25 m/s
Cut in, rated rotor speed	6.9 rpm, 12.1 rpm
Gear box ratio	97
Rated generator speed	1173.7 rpm
Rotor, Tower, nacelle mass	110 ton, 347.4 ton, 240 ton

In Section 2, the turbine model specifications plus the turbine linearized models are discussed. In Section 3, the proposed CPC design, and the controller objectives are shown. The design considers two cases; single operating point-based model, and a polytopic-based model. In Section 4, IPC design is discussed. The simulation results showing a comparison between the proposed controller and a conventional PI controller are shown in Section 5. Finally the conclusions are stated in Section 6.

## 2. Model description

Simulations are performed on a full nonlinear turbine model provided by the FAST (Fatigue, Aero-dynamics, Structures, and Turbulence) software code developed at the US National Renewable Energy Laboratory (NREL) [9]. The model used is a 3-bladed, variable-speed 5 MW wind turbine model with the specifications given in Table 1.

More specifications could be found in [10, pp. 26]. The pitch actuator, represented as a second order model, has a pitch angle range from 0 to 90° with maximum rate of 8°/s.

FAST provides many degrees of freedom reflecting whether or not different turbine parts' dynamics are considered. The following degrees of freedom (DOF) are considered in our study:

- Generator DOF ( $q_1$ ).
- Drivetrain rotational-flexibility DOF ( $q_2$ ).
- First fore-aft tower bending-mode DOF ( $q_3$ ).
- First flapwise blade mode for each blade DOF ( $q_4, q_5, q_6$ ).

where ( $q_l$ ) denotes the displacement of the  $l$ th DOF. Each DOF could be presented as a linearized model around certain operating point according to:

$$M\Delta\ddot{q}_l + C\Delta\dot{q}_l + K\Delta q_l = F^*u + F_d^*u_d \quad (1)$$

where  $M$ ,  $C$ ,  $K$ ,  $F$ ,  $F_d$ ,  $u$ , and  $u_d$  denote mass matrix, stiffness matrix, damping matrix, control input matrix, wind input disturbance matrix, control input vector, and disturbance input vector, respectively. Assume  $\Delta x = [\Delta q_l, \Delta \dot{q}_l]^T$ , the linearized model takes the form:

$$P(S) : \begin{cases} \Delta \dot{x} = A\Delta x + B\Delta u + B_d\Delta u_d \\ \Delta y = C\Delta x + D\Delta u + D_d\Delta u_d \end{cases} \quad (2)$$

where  $\Delta x$ ,  $\Delta u$ ,  $\Delta u_d$ , and  $\Delta y$  are the state vector perturbation, perturbation in the control action, perturbation in input disturbance, and perturbation in the output, respectively. Fig. 1 shows the synthesis of FAST model used in simulation.

The generator torque has four control regions: 1, 2, 2.5, and 3. Region 1 is a control region before cut in wind speed ( $v_{ci}$ ) with zero generator torque so no power is extracted from the wind. Instead, the wind is used to accelerate the rotor for start-up. The main task in Region 2 is optimizing power capture by maintaining a constant (optimal) tip-speed ratio; ( $\lambda = \lambda_0$ ), while the pitch angle is kept zero. In Region 3, the wind speed is above-rated speed. In this region, the generator controller task is to hold the generator torque constant. In the same time, the pitch controller regulates the generator speed at the rated value in order to capture the rated power. Region 2½ is a linear transition between Regions 2 and 3 used to limit tip speed (for less noise emissions) at rated power. The torque speed response of the model is shown in Fig. 2.

## 3. Designing an LMI-based collective pitch controller

The proposed technique is to design state feedback, LMI-based collective pitch controller (CPC) to regulate the generator speed in region 3. This controller is combined with IPC that mitigates the flapwise moment by canceling (1P) frequency. The proposed control strategy is shown in Fig. 3.

$M_{1,2,3}$  are the blade tip flapwise moments of each blade.  $\omega_{gen}$  is the generator speed. The total control action ( $\beta$ ) is calculated as follows:

$$\beta = \beta_{ipc} + \beta_{cpc} + \bar{\beta} \quad (3)$$

where ( $\bar{\beta}$ ) is the pitch angle operating point. It is calculated by changing operating point with wind speed through a look up table. The generator speed is regulated by the control action ( $\beta_{cpc}$ ), and the flapwise moment is reduced by the control action ( $\beta_{ipc}$ ).

In this design, we are looking for a solution that addresses the combination of the following objectives:

- Efficient disturbance rejection for better speed regulation ( $H_\infty$  problem) [11]. This could be achieved by keeping the RMS gain of  $T(s)_\infty$  ( $H_\infty$  norm) below a predefined value  $\gamma_0$ : ( $\gamma_0 > 0$ ).  $T(s)_\infty$  is the closed loop transfer function from  $W$  to  $Z_\infty$ , where  $Z_\infty = [\Delta\omega_{gen}]$  represents the regulation error due to disturbance ( $W$ ).
- To minimize a cost function ( $J$ ) that reflects a weighted sum of the control effort and states' perturbations. Trade-off between the control effort and the performance is represented as a  $H_2$  problem. [11]. The minimization is carried by keeping the  $H_2$

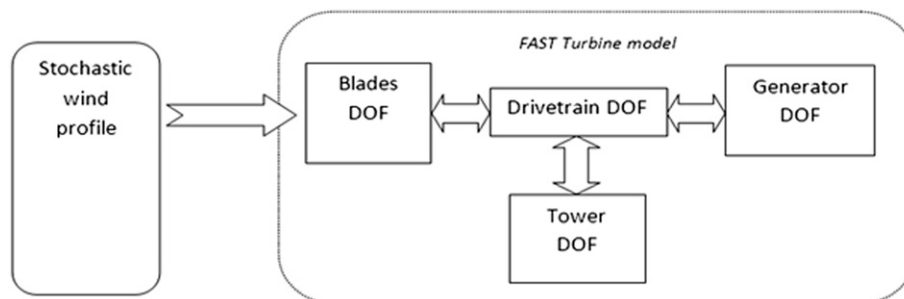


**Fig. 1.** FAST model components.

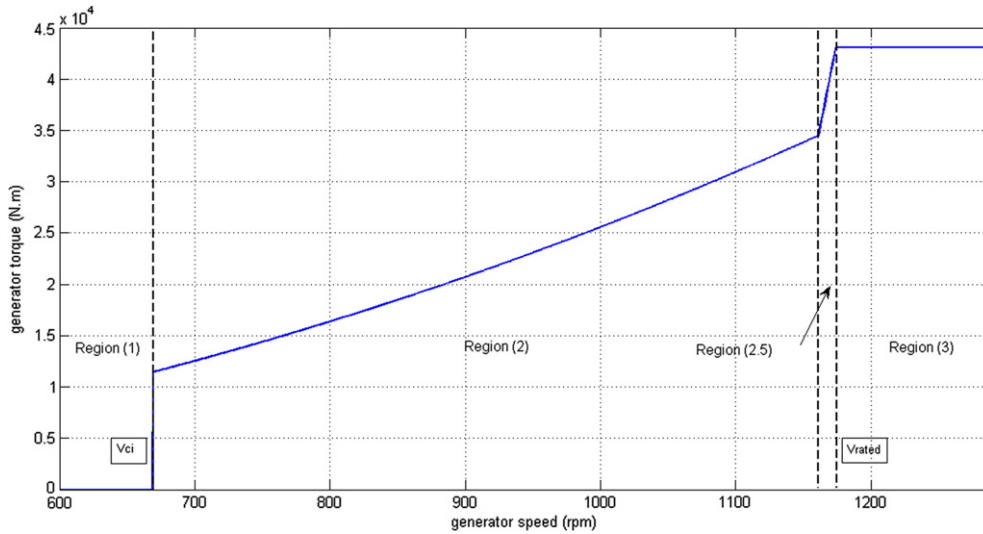


Fig. 2. Torque speed characteristics of the generator.

norm (LQG Cost) of  $T(s)_2$  below a predefined value  $v_0$ : ( $v_0 > 0$ ).  $T(s)_2$  is the closed loop transfer function from  $W$  to  $Z_2$ .  $Z_2$  is defined as:

$$(Z_2 = Q \cdot \Delta X + R \cdot \Delta u)$$

where the square matrix  $Q = \text{diag} \{Q_1, Q_2, Q_3\}$  and vector  $R$  represent the weighting terms of the LQG cost function ( $J$ ) given in Eq. (4).  $Z_2$  represents the trade-off criteria between the perturbations in states and control action according to the following objective function:

$$J = \int_0^{\infty} (Q^2 \Delta X^2 + R^2 \Delta u^2) dt \quad (4)$$

The LQG minimization problem could be used as a tool for comparison between performance and control action.

3. Achieving a desired transient response by maintaining the closed loop poles inside a particular region ( $D$ ): (pole clustering problem) [12].

Two design cases will be considered; a single operating point-based case and a polytopic-based model case.

### 3.1. Designing a CPC for a single operating point-based model

FAST can provide a linearized model in the form given in Eq. (2). This linearized model is calculated at certain operating point ( $\bar{\omega}_{gen}, \bar{\beta}, \bar{v}_w$ ) [9], where ( $\bar{\cdot}$ ) represents the operating point value of the variable ( $\cdot$ ).  $v_w$  is the hub height wind speed. In our design model, the enabled DOFs are the generator, and the drive train flexibilities DOFs. These are the only DOFs that could be observed of the measured generator speed. They are considered the dominant dynamics in our turbine [10]. As a result, the other enabled DOFs will be considered as unstructured model uncertainty.

The state vector is  $\Delta \bar{X} : \Delta \bar{X} = [\Delta X_1, \Delta X_2, \Delta X_3]^T$  where:

- (1)  $\Delta X_1$  = drivetrain rotational-flexibility (perturbations in drivetrain torsional displacement) (m);
- (2)  $\Delta X_2$  = generator DOF (perturbations in rotor speed) (rad/s); and
- (3)  $\Delta X_3$  = Drivetrain flexibility (perturbations in Drivetrain torsional velocity) (m/s).

$\Delta u = [\Delta \beta]$ ,  $\Delta u$  is the perturbation in the collective pitch (control action),  $\Delta u_d = [\Delta v_w]$  is the perturbation in the wind speed,  $\Delta y = [\Delta \omega_{gen}]$ ,  $\Delta y$  is the perturbation in generator speed. The design model  $p(s)$  is completely observable and completely controllable. It is

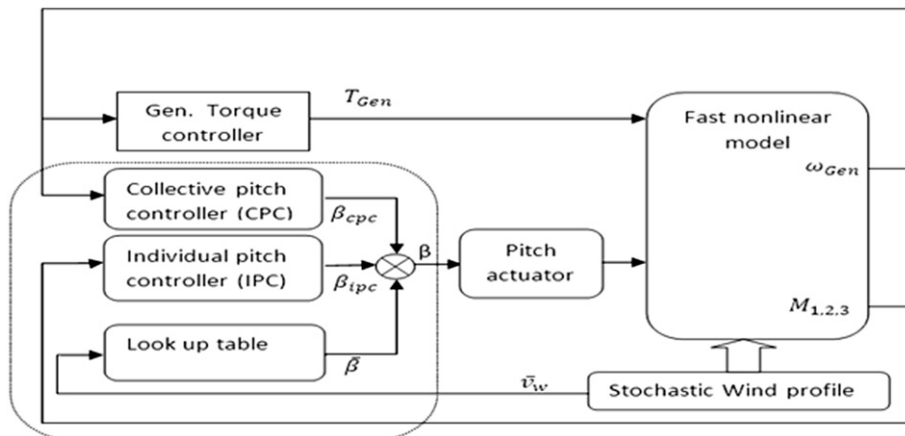


Fig. 3. The pitch controller synthesis.

a linearized model around the operating point: ( $\bar{\omega}_{gen} = \omega_{rated} = 1173.6$  rpm,  $\bar{\beta} = 14.93^\circ$ ,  $\bar{v}_w = 18$  m/s). The model could be written in the following form:

$$P(S) : \begin{cases} \Delta \dot{X} = A^* \Delta X + B_1^* \Delta W + B_2^* \Delta u \\ Z_\infty = C_1^* \Delta X + D_{11}^* \Delta W + D_{21}^* \Delta u \\ Z_2 = C_2^* \Delta X + D_{22}^* \Delta u \end{cases} \quad (5)$$

where ( $Z_\infty = \Delta y$ ) and ( $Z_2 = Q^* \Delta X + R^* \Delta u$ ). The state feedback controller takes the form:

$$\Delta u = \beta_{cpc} = K^* \Delta X \quad (6)$$

The LMI problem includes the optimization of a cost function  $f$  ( $H_\infty/H_2$  trade-off criteria)

$$f = \alpha \|T_\infty\|_\infty^2 + \beta \|T_2\|_2^2 \quad (7)$$

where  $\alpha$  and  $\beta$  are some weighting scalars.

In this design, the CPC is constructed to solve:

$$\text{minimize} (\alpha^* \gamma^2 + \beta^* \text{Trace}(Q))$$

Subject to:

$$\begin{cases} H_\infty \text{ performance} : \left\{ \begin{pmatrix} AP + PA^T + B_2 Y + Y^T B_2^T & B_1 & PC_1^T + Y^T D_{12}^T \\ * & -I & D_{11}^T \\ * & * & -\gamma^2 I \end{pmatrix} < 0 \right. \\ H_2 \text{ performance} : \left\{ \begin{pmatrix} Q & C_2 P + D_{22} Y \\ * & P \end{pmatrix} > 0 \right. \\ \text{Trace}(Q) < v_0^2 \\ \gamma^2 < \gamma_0^2 \\ \text{Pole clustering} : \left\{ \pi \otimes P + I \otimes (P^* A_{cl}) + I^T \otimes (A_{cl}^T * P) < 0 \right. \end{cases} \quad (8) - (10)$$

where  $P$  is a Lyapunov matrix that satisfies all the previous constraints, (\*) denotes symmetrical element, ( $\otimes$ ) denotes the kronecker product,  $A_{cl}$  is the state matrix of the closed loop system. ( $I, \pi$ ) are the parameters' matrices of the desired pole clustering region. Further details and proofs are given in [11,12]. Once a feasible solution for the LMI framework is reached, an optimal value of the cost function in Eq. (7) is also reached. The solution yields ( $p, Y^*, \gamma^*, Q^*$ ), where  $\gamma^*$  is the optimal  $H_\infty$  performance, and  $Q^*$  is the optimal  $H_2$  performance. This problem is considered a semi-definite problem (SDP). LMI Lab solver in LMI control toolbox [13] is used to solve this problem. The final state feedback controller is calculated as:

$$K = Y^* (P)^{-1} \quad (11)$$

The values of  $\gamma_0$  and  $v_0$  are chosen as:

$$\gamma_0 = 17.3, v_0 = 1$$

The criteria behind that choice were that these values should be as small as possible for better performance while a feasible solution is obtained.

#### a. Pole clustering regions

Pole clustering regions are chosen to guarantee improvement in transient response. This can be achieved by specifying regions representing limits on the system's eigenvalues. The first region ( $R_1$ ) guarantees an upper limit on settling time. The second

region ( $R_2$ ) guarantees a lower limit on settling time (which prevents excessive control action). Finally region three ( $R_3$ ) is chosen as an upper bound on damping ratio. The previous regions are convex subsets of the complex plane characterized by [14]:

$$D = \{z \in \mathbb{C} : \pi + I z + I^T \bar{z} < 0\} \quad (12)$$

$R_1$  and  $R_2$  regions are defined by a vertical strip between ( $h_1, h_2$ ) with characteristic function ( $F_{D1,2}$ ) as:

$$F_{D1,2}(Z) = \begin{pmatrix} 2h_1 - (z - \bar{z}) & 0 \\ 0 & (z + \bar{z}) - 2h_2 \end{pmatrix} \quad (13)$$

Region ( $R_3$ ) is a conic sector centered at the origin with inner angle ( $2\theta$ ) as shown in Fig. 4. The characteristic function ( $F_{D3}$ ) is given as:

$$F_{D3}(Z) = \begin{pmatrix} \sin(\theta)^*(z + \bar{z}) & -\cos(\theta)^*(z - \bar{z}) \\ \cos(\theta)^*(z - \bar{z}) & \sin(\theta)^*(z - \bar{z}) \end{pmatrix} \quad (14)$$

The region parameters are taken as  $h_1 = -1$ ,  $h_2 = -4$ ,  $\theta = 80^\circ$  (compatible with the system dynamics) [1].

The resulting LMI region ( $D$ ) is the intersection of the three regions stated above as shown in Fig. 4.

#### b. $H_\infty/H_2$ trade-off criteria

The relation between ( $H_\infty$  performance/ $H_2$  performance) is calculated at different weights ( $\beta, \alpha$ ) of the trade-off criteria given in (Eq. (7)). Fig. 5 shows the relation between  $H_\infty$  performance and  $H_2$  performance.

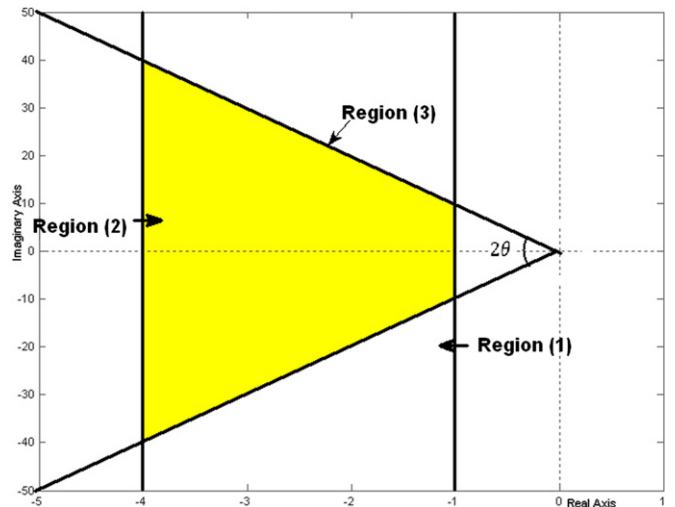


Fig. 4. Pole clustering regions.

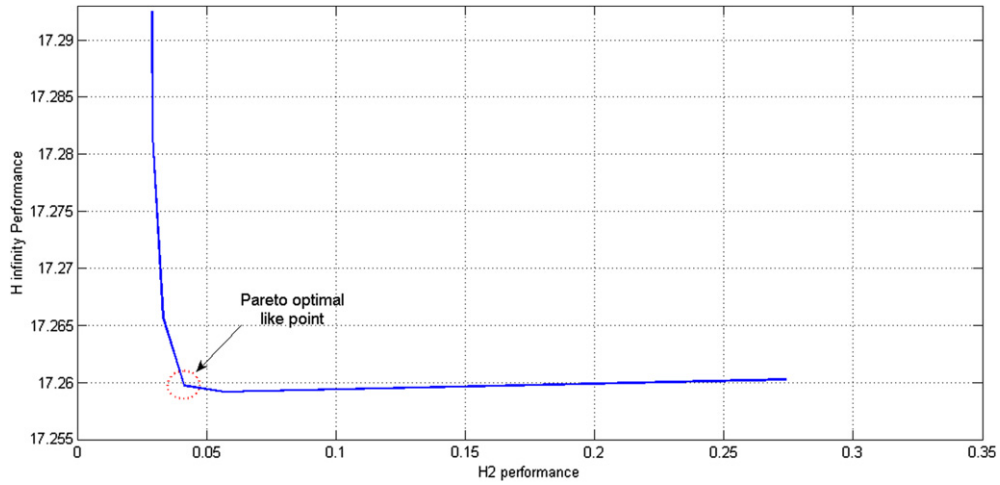


Fig. 5.  $H_\infty$  performance/ $H_2$  performance relation.

The optimal performance occurs at the minimum value of the cost function (Eq. (7)). This value exists as a Pareto-optimal-like point which is circled in Fig. 5. The weights for the cost function  $f$  in Eq. (7) that achieve the Pareto-optimal-like point are  $\beta = 47$ , and  $\alpha = 0.1$ .

Now, the LMI problem could be written in this form:

$$\begin{aligned} & \text{minimize } f : (f = 0.1 * \|T_\infty\|_\infty^2 + 47 * \|T_2\|_2^2), \\ & \text{subject to } \begin{cases} \|T_\infty\|_\infty < 17.3 \\ \|T_2\|_2 < 1 \\ \text{closed loop poles}(A_{cl}) \in \text{region}(D) \end{cases} \end{aligned} \quad (15)$$

Solving for the controller's gains yields:  
 $K_1 = [674.6 \quad 8.024 \quad 5.7]^T$

where  $K_1$  is the controller's gain for the single operating model-based case. Fig. 6 depicts the resultant closed loop poles for different operating points (different wind speeds) using the previous controller  $K_1$ . Fig. 6 shows that the controller manages

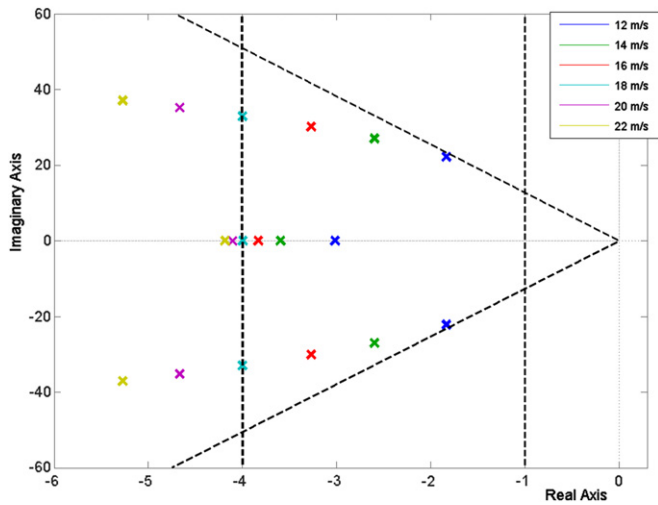


Fig. 6. Closed loop poles in single design model case.

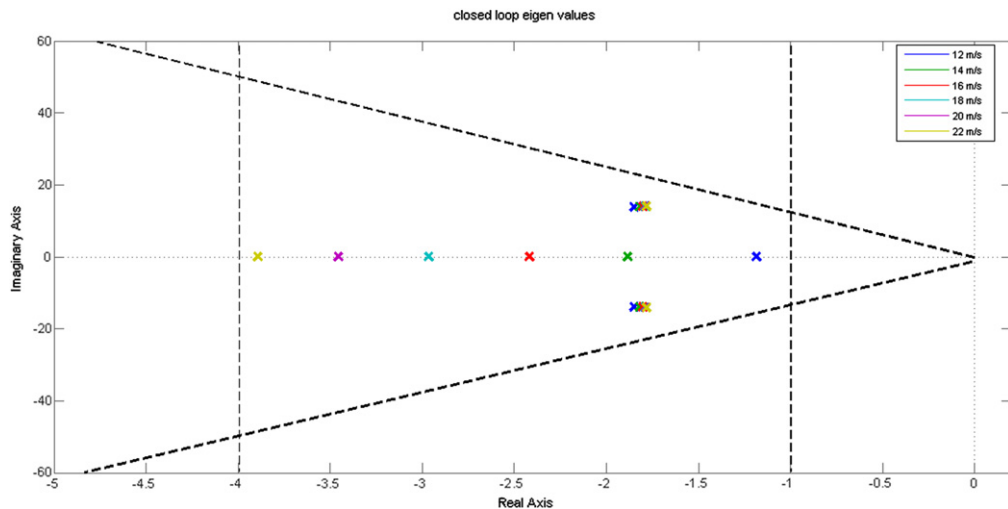


Fig. 7. Closed loop poles in polytopic model case.

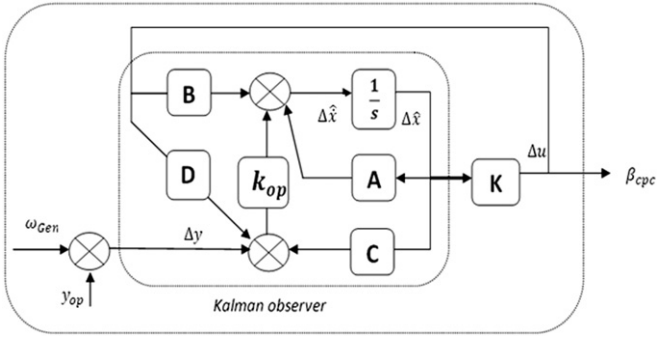


Fig. 8. Kalman observer structure.

to keep the eigenvalues at the desired region ( $D$ ) only at certain operating points. At wind speeds above 18 m/s (design operating point), the closed loop poles are outside the predefined pole clustering region ( $D$ ). This is attributed to the fact that the design is based on single design model.

For the cases where the resultant closed loop eigenvalues are outside region ( $D$ ), the controller ( $K_1$ ) will lead to excessive control action. This might lead to undesired actuator saturation. In addition to actuator saturation, amplification of unstructured dynamics of parts of the system like blades, tower, and platform is feared. Thus, this controller, in general, is not recommended for the actual nonlinear system. The need for a better controller requires the study of a polytopic model of the system.

model represents a different operating point with a unique pitch angle ( $\bar{\beta}$ ). All the models are linearized at the same generator speed which is equal to the rated speed ( $\bar{\omega}_{gen} = \omega_{rated}$ ). The  $i$ th model  $P_i(S)$  could be represented in the form:

$$P_i(S) : \begin{cases} \Delta \dot{X} = A_i^* \Delta X + B_{1i}^* \Delta W + B_{2i}^* \Delta u \\ Z_\infty = C_{1i}^* \Delta X + D_{11i}^* \Delta W + D_{12i}^* \Delta u \\ Z_2 = C_{2i}^* \Delta X + D_{2i}^* \Delta u \end{cases} \quad (16)$$

In this case the fixed polytope is surrounded by a convex envelope  $\Omega$ . This envelope has six vertices.  $\Omega$  is defined as:

$$\Omega = \text{Co}\{S_1, S_2, \dots, S_6\} = \left\{ \sum_{i=1}^6 \alpha_i S_i : \alpha_i \geq 0, \sum_{i=1}^6 \alpha_i = 1 \right\} \quad (17)$$

where  $\text{Co}$  represents the set of vertices defining the set ( $\Omega$ ), and each system matrix  $S_i$  is defined as:

$$S_1 = \begin{bmatrix} A_1 & B_{11} & B_{21} \\ C_{11} & D_{111} & D_{121} \\ C_{21} & 0 & D_{21} \end{bmatrix}, S_2 = \begin{bmatrix} A_2 & B_{12} & B_{22} \\ C_{12} & D_{122} & D_{122} \\ C_{22} & 0 & D_{22} \end{bmatrix}, \dots, S_6 = \begin{bmatrix} A_6 & B_{16} & B_{26} \\ C_{16} & D_{126} & D_{126} \\ C_{26} & 0 & D_{26} \end{bmatrix}$$

The polytopic-based model has the following LMI formula:

$$\text{minimize} (\alpha^* \gamma^2 + \beta^* \text{Trace}(Q))$$

Subject to:

$$\left\{ \begin{array}{l} H_\infty \text{ performance : } \begin{pmatrix} A_i P + P A_i^T + B_{2i} Y + Y^T B_{2i}^T & B_{1i} & P C_{1i}^T + Y^T D_{12i}^T \\ * & -I & D_{11i}^T \\ * & * & -\gamma^2 I \end{pmatrix} < 0 \\ H_2 \text{ performance : } \begin{pmatrix} Q & C_{2i} P + D_{22i} Y \\ * & P \end{pmatrix} > 0 \\ \text{Trace}(Q) < \nu_0^2 \\ \gamma^2 < \gamma_0^2 \\ \text{Pole clustering : } \pi \otimes P + \Gamma \otimes (P^* A_{cli}) + \Gamma^T \otimes (A_{cli}^T * P) < 0 \end{array} \right. \quad (18-20)$$

### 3.2. Designing a CPC for a polytopic-based model

The single model-based controller proposed in the previous section has already shown a drawback in performance. Thus, a selection of different operating points' models must be taken into consideration. The different operating points cover the range of wind speeds of region 3. Six different linearized design models at different wind speeds are considered; these models are taken at ( $\bar{v}_w = 12$  m/s, 14 m/s, 16 m/s, 18 m/s, 20 m/s, 22 m/s). Each

where ( $i = 1, 2, \dots, 6$ ).

Here we are seeking for a single quadratic Lyapunov function ( $P$ ). It should fulfill all the design objectives mentioned in Eq. (15) for all plants in the polytope.

Solving for the controller's gains yields:

$$K_2 = [3.5842 \quad 2.0471 \quad 1.6246]^T$$

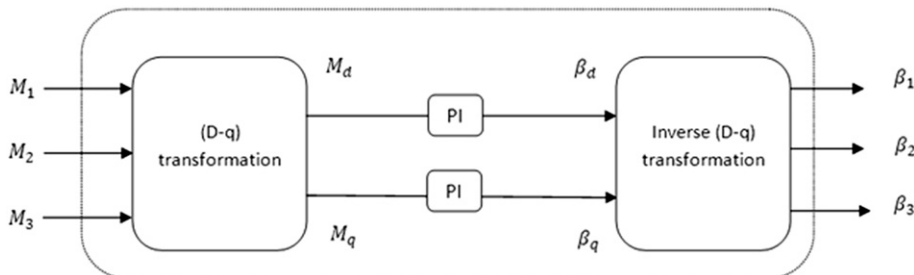


Fig. 9. IPC structure.

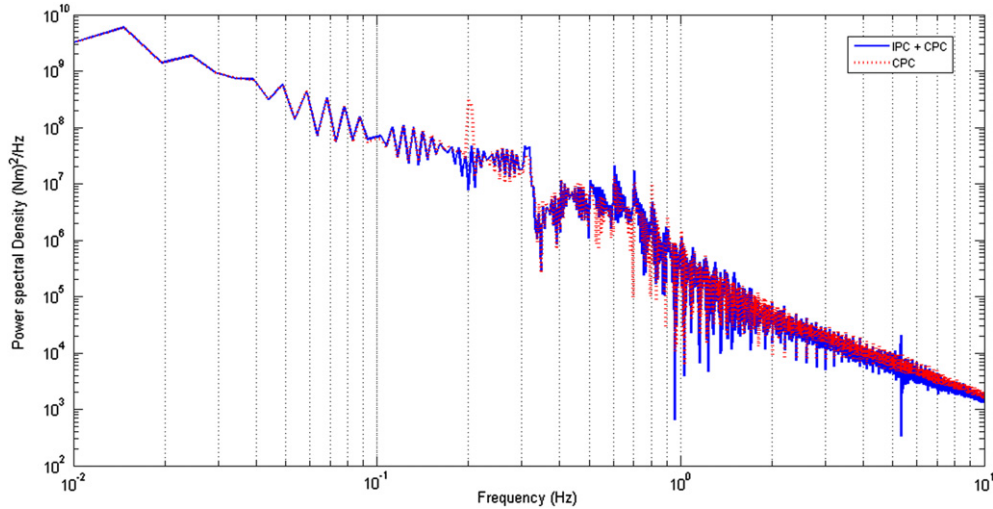


Fig. 10. Flap blade rotor bending moment.

Fig. 7 depicts the resultant closed loop poles for different operating points (different wind speeds) using the previous controller ( $K_2$ ). Fig. 7 shows that  $K_2$  managed to keep all the eigenvalues inside the desired region ( $D$ ) at all operating points.

### 3.3. Designing states observer

CPC is a state feedback controller. As some states are not measurable, an optimal observer (Kalman filter) is designed according to [15]. For designing a Kalman observer, disturbance and noise variance data must be available. According to the linearized model in Eq. (2), the disturbance in our case is the perturbation in the wind speed around certain operating point. In region 3 perturbation in wind speed ranges from 12 to 24 m/s. The observer is based on a linearized model derived at wind speed of 18 m/s (mean wind speed). Assuming a Gaussian probability distribution for the wind speed, then the probability of existence in the previous range equals (99%) if this range represents ( $6^* \sigma$ ); where  $\sigma$  is the standard deviation of the wind speed. As a result the variance in disturbance could be calculated as:

$$Q = \sigma^2 = E(WW^T) = 4, R = E(NN^T) = 0.01$$

where  $W$  represents the process disturbance,  $N$  represents the measurement noise; its variance is taken as 1% of the measured generator speed. The correlation between noise and disturbance is assumed to be zero. The observer model using Kalman observer is:

$$\Delta \hat{x} = A\Delta \hat{x} + B\Delta u + K_{ob}(\Delta y - c\Delta \hat{x} - D\Delta u) \quad (21)$$

The covariance matrix of the estimated state error is calculated as:

$$p_{op} = \lim_{t \rightarrow \infty} (E((\Delta x - \Delta \hat{x}) * (\Delta x - \Delta \hat{x})^T)) \quad (22)$$

where  $K_{ob}$  is the Kalman filter which is founded by solving algebraic Riccati equation. The optimal solution could be reached using:

$$K_{ob} = (p_{op}C^T + \bar{N})\bar{R}^{-1} \quad (23)$$

where  $\bar{R} = R + D_d Q D_d^T$ ,  $\bar{N} = B_d Q D_d^T$ . Kalman observer's structure is shown in Fig. 8.

### 4. Individual pitch controller design

To reduce the periodic blade flapwise moment, periodic individual pitching technique of the rotor blades are proposed (see e.g. [2,16]). In this approach, each of the blades needs to be pitched according to the intermittent loads that it experiences. The spectrum of the blade root bending moment caused by wind shear has a dominant component at frequency (1p) while higher harmonics could be damped [17]. However, there are some methods for reduction of higher load harmonics (called higher harmonic control HHC) as mentioned in [18]. At the same time the rotor speed regulation is unaffected due to the decoupling between individual and collective pitch control [17]. As a result, load mitigation paid price is the increase in the actuator activity. This control action has frequency of 1p (typically 0.2 Hz in our case), that's why it does not impose magnificent pressure on the pitch actuator. It also requires measuring the flapwise moment of each blade plus the rotor's azimuth angle. IPC synthesis is shown in Fig. 9.

This controller requires the measurement of the blade tip flapwise moment of each blade ( $M_{1,2,3}$ ). These periodic loads are transformed to a  $D$ - $q$  frame by (park's  $d$ - $q$  transformation [2]) as:

$$\begin{pmatrix} M_d \\ M_q \end{pmatrix} = \frac{2}{3} \begin{pmatrix} \cos(\psi) & \cos(\psi + \frac{2\pi}{3}) & \cos(\psi + \frac{4\pi}{3}) \\ \sin(\psi) & \sin(\psi + \frac{2\pi}{3}) & \sin(\psi + \frac{4\pi}{3}) \end{pmatrix} \begin{pmatrix} M_1 \\ M_2 \\ M_3 \end{pmatrix}, \quad (24)$$

where  $M_d$ ,  $M_q$ ,  $\psi$  are the direct (tilt) moment, quadratic (yaw) moment, and the rotor azimuth angle, respectively. The tilt and yaw

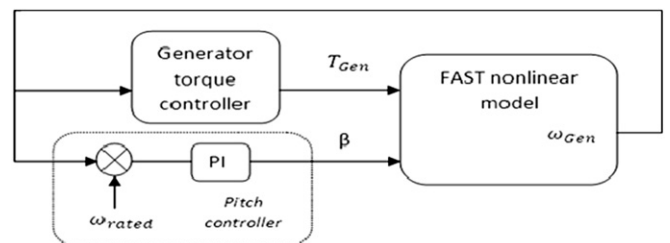
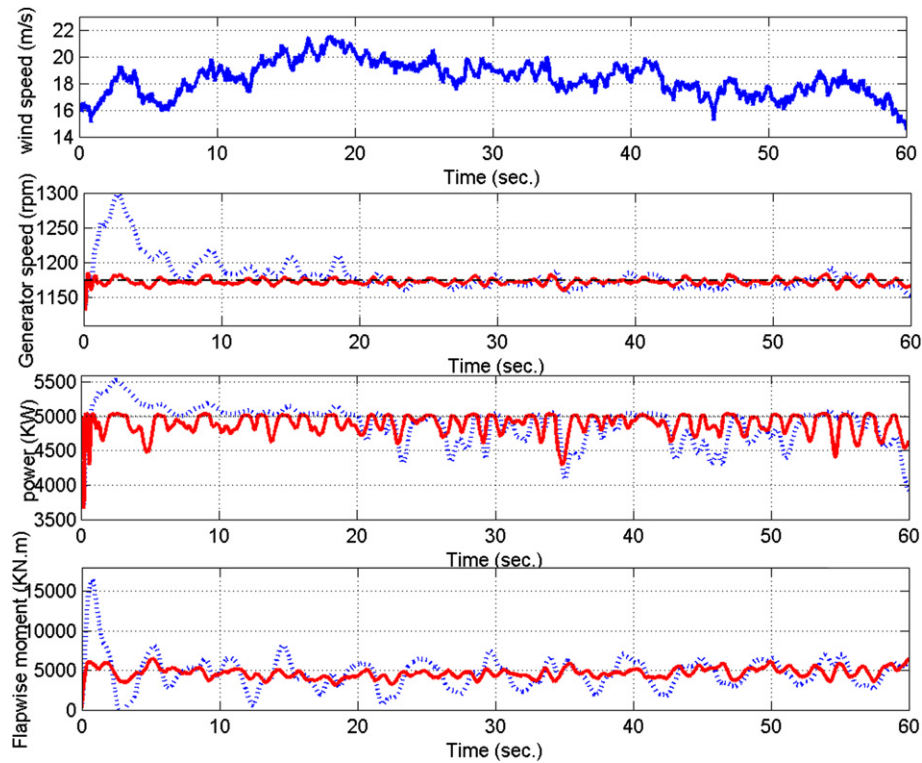


Fig. 11. Classic collective pitch PI controller synthesis.



**Fig. 12.** PI (dashed line) controller versus LMI pitch controller (solid line): (a) hub height wind speed (m/s), (b) generator speed (rpm), (c) electrical power (kW), and (d) flapwise moment (KN m).

moments are regulated by PI controllers. The PI controller gains are fine tuned to give the appropriate control action needed to cancel the fatigue load without affecting the speed regulation. The resulting control action  $\beta_d, \beta_q$  referred to the  $(D-q)$  frame. Last step will be transforming the control action to the rotating frame again by the inverse transformation (2/3 transformation):

$$\beta_{ipc} = \begin{pmatrix} \beta_1 \\ \beta_2 \\ \beta_3 \end{pmatrix} = \begin{pmatrix} \cos(\psi) & \sin(\psi) \\ \cos\left(\psi + \frac{2\pi}{3}\right) & \sin\left(\psi + \frac{2\pi}{3}\right) \\ \cos\left(\psi + \frac{4\pi}{3}\right) & \sin\left(\psi + \frac{4\pi}{3}\right) \end{pmatrix} \begin{pmatrix} \beta_d \\ \beta_q \end{pmatrix} \quad (25)$$

Comparison of the flapwise moment spectral before and after using IPC for a turbine experiencing a stochastic wind profile is shown in Fig. 10. As shown, IPC managed to reduce the (1p) component significantly (which is represented at frequency 0.2 Hz). As a result, the fatigue moment affecting the blade and the nacelle will be reduced also dramatically.

**Table 2**  
Speed and power comparison.

		Conventional PI	LMI-based
Generator speed (as a percentage of the rated speed)	Max.	110.7%	101.1%
	Mean	100.7%	99.91%
	Std. dev.	24 rpm	4 rpm
Electric power (as a percentage of the rated power)	Max.	110.56%	101%
	Mean	97.84%	98.26%
	Std. dev.	271 kW	151 kW

## 5. Simulation results

The proposed controller is tested using FAST nonlinear model. Two uncertainties will be tested. The first is a stochastic wind model profile applied to the turbine. This wind profile covers all operating points. It represents a perfect disturbance to test the controller performance under severe conditions. The turbine model will be tested against stochastic full field wind profile developed by the NREL TurbSim wind simulator [19]. The second is an unstructured model uncertainty represented by enabling more degree of freedoms in FAST model. Although our controller is based on 2 DOFs design model, it will be tested using a nonlinear model with 6 DOFs (see Section 2).

The proposed controller performance will be compared to a conventional collective pitch PI controller. This controller is tuned to guarantee good speed regulation. The controller parameters are ( $k_p = 0.0018$ ,  $k_i = 0.001779$ ). The controller is based on single linearized model derived at the average wind speed ( $v_w = 18$  m/s). Fig. 11 shows the structure of the classic collective pitch PI controller.

Comparison between the traditional PI controller (dashed line) and the proposed controller (solid line) is shown in Fig. 12. A through comparison between the two controllers is given in Tables 2 and 3.

**Table 3**  
Flapwise moment comparisons.

		PI (KN m)	IPC
Flapwise moment	Max	16460	6447
	Std. dev.	2129	649

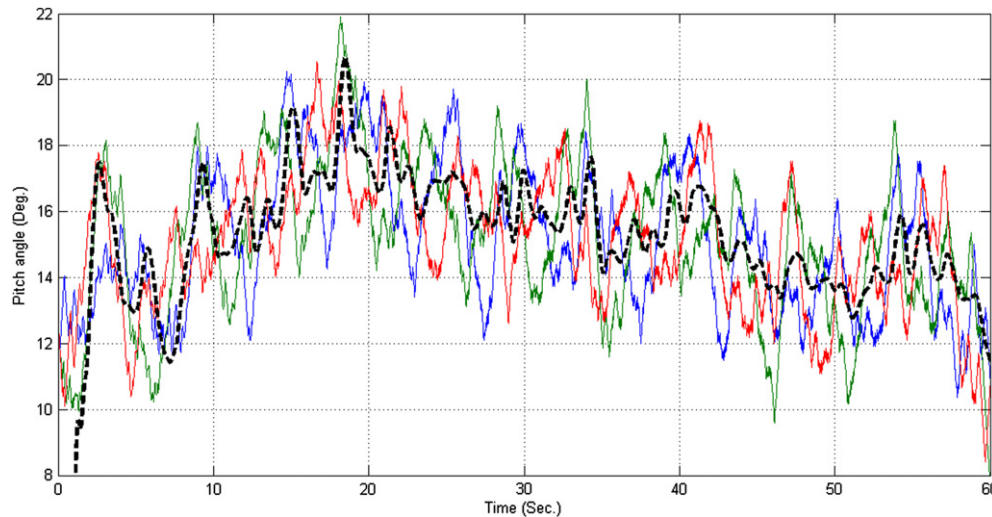


**Fig. 13.** Pitch angle in PI CPC case (dashed line), in the proposed IPC case (solid line: blue, green, and red for blade 1, 2, 3, respectively). (For interpretation of the references to colour in this figure legend, the reader is referred to the web version of this article.)

Table 2 shows a comparison of the speed regulation and harvested power for the two controllers; the conventional PI and the proposed LMI-based controller.

Table 2 shows that the LMI controller gives better speed regulation as it has managed to reduce the speed standard deviation significantly (6 times less). It has also reduced the generator's maximum speed. This will prevent the mechanical overload on the drive train, and thus increasing the machine's life time. On the other hand, the mean harvested power has improved slightly, but the maximum power has reduced significantly. This prevents the false shut down of the generator due to overloading, and keeps it working within permissible rated values. Flapwise moment is compared for the two controllers in Table 3.

The comparison shows the privilege of using the proposed (IPC) controller. The conventional PI controller is a collective pitch controller; it cannot reduce the cyclic mechanical fatigue loads. The IPC has managed to reduce the cyclic loads significantly by alleviating the (1P) frequency loads. The strong standard deviation reduction ensures this (four times less). More important, the IPC has managed to reduce the maximum load significantly, and this will keep the flapwise moment in a safe-side range of operation according to the turbine dynamics constraints stated in [1]. Thus, the maintenance cost will be diminished, and the lifetime of the turbine will increase.

The control action for the two controllers is shown in Fig. 13. The comparison shows that the proposed controller exerts control effort that is slightly more than the PI controller. This extra control effort is necessary for mitigating the fatigue loads. Moreover, the control action of the proposed controller is within the permissible actuator limits.

## 6. Conclusion

This paper has addressed the problem of designing an LMI-based robust CPC for large variable-speed variable-pitch wind turbines. The CPC is integrated with IPC to reduce the mechanical loads. CPC has been first designed based on single operating point-based model, but the desired constraints were not met at all operating points. A polytopic model-based approach has been considered to overcome this issue. The design constraints have included  $H_\infty$  problem,  $H_2$  problem,  $H_\infty/H_2$  trade-off criteria, plus pole clustering.

The performance of the proposed controller has been compared to a classical collective pitch PI controller. The comparison has shown

that the proposed LMI-based controller has achieved improvements in performance in terms of mechanical load reduction, speed regulation, and full load power harvesting. The results show that the speed regulation has improved by six folds; Fatigue load fluctuation has reduced 4 times than the conventional PI controller.

## References

- [1] Jonkman JM. Dynamics modeling and loads analysis of an offshore floating wind turbine. Technical report, NREL/TP-500-41958; November 2007.
- [2] Bossanyi EA. Individual blade pitch control for load reduction. *Wind Energy*; 2003;119–28.
- [3] Geyler M, Caselitz P. Individual blade pitch control design for load reduction on large wind turbines. *Proceedings of the European Wind Energy Conference, Milan, Italy; 2007*, p. 82–86.
- [4] Laks JH, Pao LY, Wright A. Combined feed forward/feedback control of wind turbines to reduce blade flap bending moments. In: *AIAA/ASME wind energy symposium, Orlando, FL; 2009*.
- [5] Fiona Dunney, Lucy Y. Paoz, Alan D. Wrightx, Bonnie Jonkman, Neil Kelle. Combining standard feedback controllers with feed forward blade pitch control for load mitigation in wind turbines. In: *Proceedings of the 48th AIAA aerospace sciences meeting, Orlando, FL, AIAA-2010-250*; Jan. 2010.
- [6] Selvam K, Kanev S, vanWingerden JW, van Engelen T, Verhaegen M. Feedback feed forward individual pitch control for wind turbine load reduction. *Int J Robust Nonlinear Control*; 2008.
- [7] Wilson DG, Berg DE, Resor BR, Barone MF, Berg JC. Combined individual pitch control and active aerodynamic load controller investigation for the 5MW upwind turbine. In: *AWEA WINDPOWER 2009 Conference and Exhibition, Chicago, Illinois; May 4–7, 2009*.
- [8] Lescher F, Zhao JY, Martinez A. Multi objective  $H_\infty/H_2$  control of a pitch regulated wind turbine for mechanical load reduction. In: *Proceedings of the european wind energy conference (EWEC), Athens, Greece; 2006*.
- [9] Jonkman JM, Buhl Jr ML. FAST users guide. NREL/EL-500-38230. Golden, CO: National Renewable Energy Laboratory; August 2005.
- [10] Jonkman J, Butterfeld S, Musial W, Scott G. Definition of a 5-MW reference wind turbine for offshore system development. NREL/TP-500-38060. Golden, CO: National Renewable Energy Laboratory; February 2009.
- [11] Zou Kemin. *Essentials of robust control*. Prentice Hall; 1997.
- [12] Chilali M, Gahinet P.  $H_\infty$  design with pole placement constraints: an LMI approach. *IEEE Trans Automat Contr*; 1996;358–67.
- [13] Pascal Gahinet, Arkadi Nemirovski, Alan J. Laub, Mahmoud Chilal. *LMI control toolbox user's guide*; 1995.
- [14] Chilali M, Gahinet P. Robust pole placement in LMI regions. *IEEE Trans Automat Contr*; Dec. 1999;2257–69.
- [15] Lewis F. *Optimal estimation*. John Wiley & Sons, Inc; 1986.
- [16] Selvam K. *Individual pitch control for large scale wind turbines*. The Netherlands: ECN; 2007.
- [17] Jelavić Mate, Petrović Vlaho, Perić Nedjeljko. Estimation based individual pitch control of wind turbine. *Automatika* 2010;51:181–92.
- [18] Bossanyi EA. Further load reductions with individual pitch control. *Wind Energy* July 2005;8:481–5.
- [19] Kelley ND, Jonkman BJ. Overview of the TurbSim stochastic in flow turbulence simulator. NREL/TP-500-41137, Golden, CO; April 2007.